Tailoring the Pressure-drop in Multi-layered Open-cell Porous Inconel Structures

Manufacturing Research Division
Faculty of Engineering
University of Nottingham, UK, NG7 2RD

Hatem Oun, Andrew Kennedy

Email: Epxho1@nottingham.ac.uk
Telephone: +44(0)1159513744
Fax: +44(0)1159513800

Abstract

This study investigates the pressure-drop behaviour associated with airflow through bulk and structurally tailored multi-layered, open-cell porous Inconel structures over a wide airflow velocity range (0-50 m s^{-1}). The effect of airflow velocity on the pressure-drop behaviour as a function of the sample thickness is presented and related to the flow behaviour corresponding to the relevant flow regimes (Darcy, Forchheimer, Turbulent and Post-turbulent). Entrance effects are highlighted as a source of the pressure-drop increase for porous structures with air gaps, regardless of their sizes, as long as they are larger than those generated by loosely-stacked structures. The pressure-drops for gapped porous structures and the mathematical-summation of the pressure drop for the corresponding individual components, were in very good agreement, at lower airflow velocities. The potential for mass-efficient porous structures, providing a high pressure-drop, was demonstrated using multiple thin porous laminates separated by air gaps.

Keywords: Single-phase flow/ Inconel multi-layer porous structures/ thickness effect/ material-efficient structures/ air gap effect

1. Introduction

The pressure-drop across open-cell porous metals is an essential consideration in the design of components for applications such as catalytic converters, filters, air-oil separators, breather plugs and heat exchangers. More commonly the pressure drop is sought to be minimised, but many applications may require the pressure drop to be tailored along the length of a complex system or to be maximised to give a "*sealing*" effect and often with the additional constraints of volume or mass efficiency.

The pressure-drop across monolithic (bulk) porous metals has been widely investigated, including studies reported in [1-6]. In many engineering systems, for low (laminar) flow velocities, the relationship between pressure-drop and airflow velocity is ably described by the Hazen-Darcy or Forchheimer equation [3, 7, 8].

The route to tailoring the pressure drop characteristics lies, however, in developing multi-layered porous structures but in this regard, porous structures made from stacked layers of porous metals have not been given much attention in the literature. Among these limited studies it has been shown [3, 2] that there is an increase (of up to 33% [3]) in the pressure drop when stacking multiple foam discs, compared with a single disc of the same total thickness. This increase was attributed to the effect of the misalignment and discontinuity in the structure where pores in the different discs might not align, with some pores facing ligaments and solid surfaces [2]. It was also considered that additional entrance effects (air flow disturbance as air goes from a large tube into multiple small channels) might occur because of the gaps between loosely-stacked structures.

This study aims to improve the understanding of the contribution of multiple interfaces across the flow direction on the pressure drop behaviour for multi-layered porous metal structures. The knowledge gained will be used to help understand the complex pressure-drop behaviour within porous structures with single and multiple air-gaps and aid in the design of material-efficient structures with tailored pressure drop characteristics.

2. Materials and Methods

2.1. Materials

Porous metal samples, with a nominal cell size of 450 μm (A-450 grade), made from an Inconel 625 alloy were provided by Alantum Europe. Samples up to 20 mm in thickness were made from multiple 1.6 mm thick porous sheets, diffusion bonded together to form open-celled porous structures as illustrated in Fig. 1.

The porous metal samples were characterised using a number of imaging and morphological measurement techniques. Information like cell morphology was provided by Scanning Electron Microscopy (SEM), using a Philips XL30 CP Scanning Electron Microscope, and X-ray micro computed tomography (CT), using a Scanco 40 instrument. Pore size was measured using Mercury Intrusion Porosimetry (MIP), utilizing an AutoPoreIV-9500 instrument from Micromeritics. Fuller characterisation of these porous structures is provided in [9].

Fig. 1 Illustration of the multi-layered porous sheet structure before bonding

2.2. Sample preparation and Pressure drop measurement

The pressure drop across porous metal samples was accurately measured over a wide range of compressed air velocities using a specifically-designed and built experimental setup (the details of which are described in [9]). In brief, it consists of a manual control valve, pressure regulator and filter, needle valve, variable area flow meter, and middle assembly (test section) in sequence as shown in Fig. 2. The specifications of the parts used along with dimensions, associated accuracies and thermal errors are given in [9].

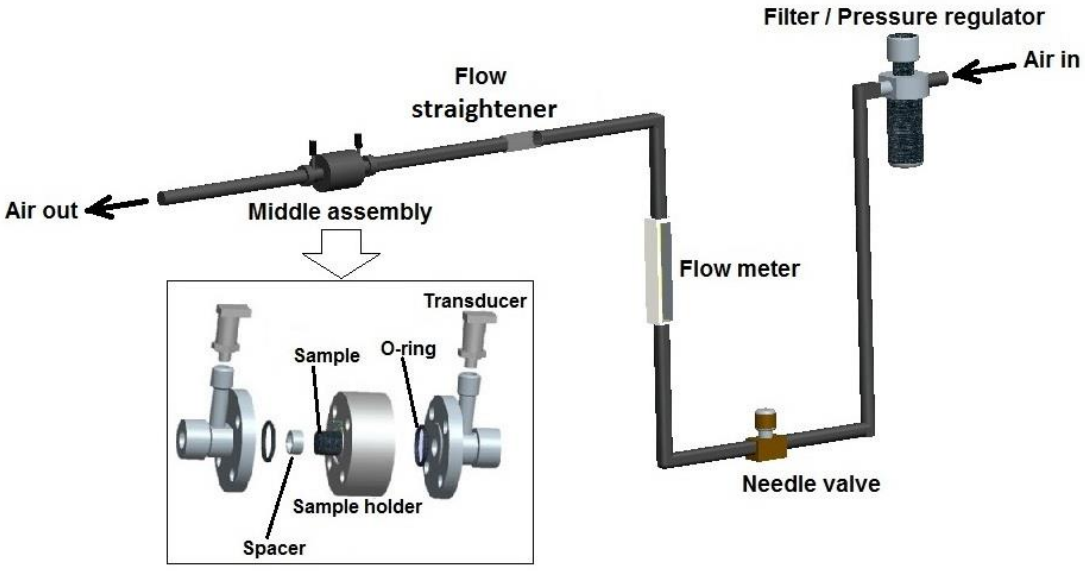

Fig. 2 Schematic drawing of the experimental set-up used in this study

The test section was designed so it can hold 25±0.2 mm diameter samples (nominal flow diameter of 21.183 mm after securing the sample with a spacer as shown in Fig.2) with different thicknesses up to 30 mm. To avoid any air passing between the sample's perimeter and the internal wall of the sample

holder, it was wrapped circumferentially with PTFE tape. The mid-assembly was then secured in place and pressure transducers were fitted as described in [9]. For all tests, the input pressure was regulated and the airflow velocity was varied depending on the test conditions. A stabilisation period was adopted to avoid any fluctuation. Pressure readings were collected using Labview software powered data logger connected to a PC. A maximum of 5% standard deviation in the results was achieved according to repeatability testing described in [9].

Porous metal samples were accurately cut to size using Electrical Discharge Machining (EDM). Porous metal samples were separated with air gaps by placing spacers of pre-determined thicknesses (with 25 mm outer diameter and 21.183 mm inner diameter) between the porous metal discs. In both cases, with and without an air gap, samples were secured inside the sample holder using spacers of an exact thickness to avoid any vibration or movement of the sample.

Compressibility effects, manifested as gas density changes, were taken into consideration when calculating the pressure drop. Even at low velocities, the pressure drop across porous metal samples is normally high enough to create these effects [7, 9]. In accordance with [7], Eq-1 was used to calculate the pressure-drop:

$$\Delta P = \frac{P_i^2 - P_o^2}{2P_r} \qquad \text{Eq-1}$$

where P_i and P_o are the absolute pressure upstream and downstream of the test section, respectively. P_r is reference pressure, which is taken as atmospheric pressure [7].

3. Results and discussion

3.1. Sample characterisation

The porous metals used in this work have a reticulated structure of interconnected pores as shown in the SEM images in Fig. 3, which also differentiates the cells from the pores. The alloying process used to manufacture Inconel porous metals from pure nickel porous structures (Fig. 3-a) results in a rough surface as illustrated in Fig. 3-b and 3-d. The cross section of the triangular struts is shown in Fig. 3-d. Struts forming the interconnected structure of the material are hollow as a result of the burn out of the PU template used to make the porous metal. The 2-D micro-CT image in Fig. 3-c, clearly shows these hollow struts.

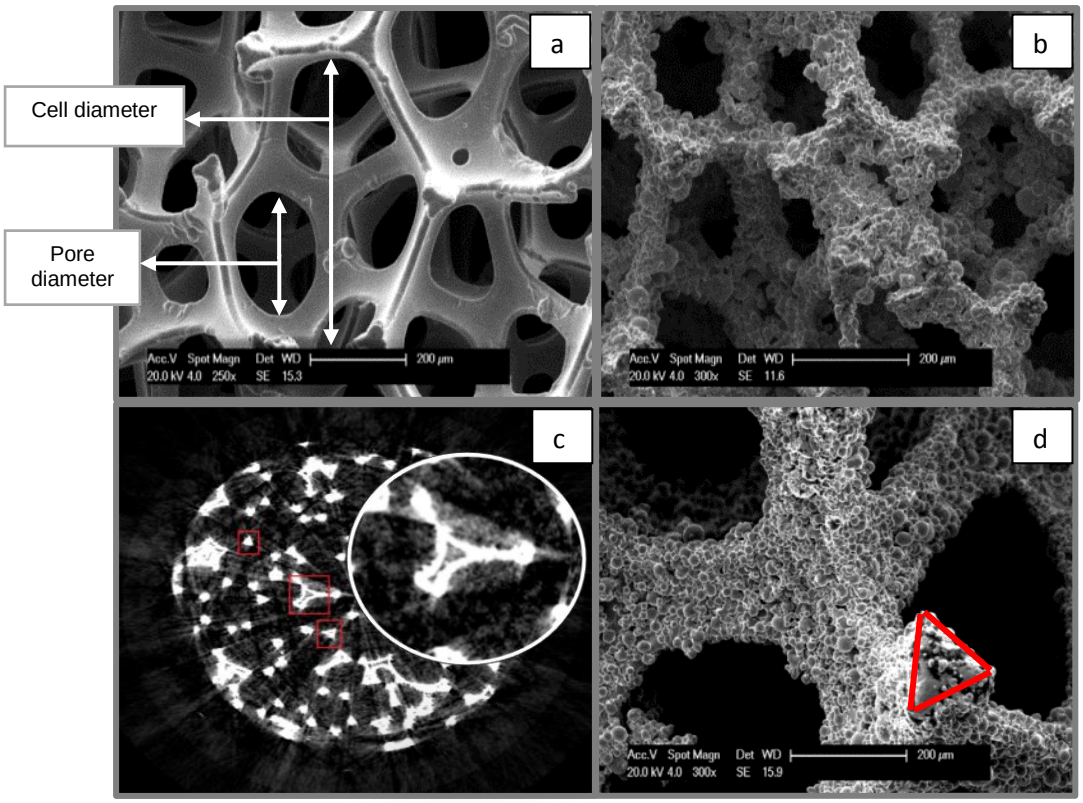

Fig. 3 a) Pure nickel porous metal before the alloying process b) Inconel porous metal c) 2-D micro-CT image of hollow struts of the porous metals d) strut triangular cross-section

Structural parameters for the porous metal are shown in Table 1. Because of the relatively thick layers of alloying element powders applied when converting porous Ni to Inconel, the actual cell size tends to be smaller than the nominal value, which refers to the initial cell diameter of the pure nickel substrate used as a template to manufacture the porous Inconel sheets.

Table 1 Porous metal structural characteristic

Property	Equipment	A-450
Nominal cell size (μm)		450
Cell size (μm)	SEM	360
Pore size (μm)	MIP	214
Density (kg m^{-3})		828
Total porosity (%)		88.0

3.2. Length-normalised pressure drop and regime change

Pressure-drop measurements were carried out on a 20 mm thick sample over an approximate air velocity range of 0 to 50 m s^{-1}. Figure 4 presents the length-normalized pressure drop versus Darcian velocity relationship. As expected, the pressure-drop increases with increasing airflow velocity in similar trends to those reported in [2, 4, 6, 7, 10-14], but a third order (rather than second order) polynomial provides a better fit to the data over the entire velocity range.

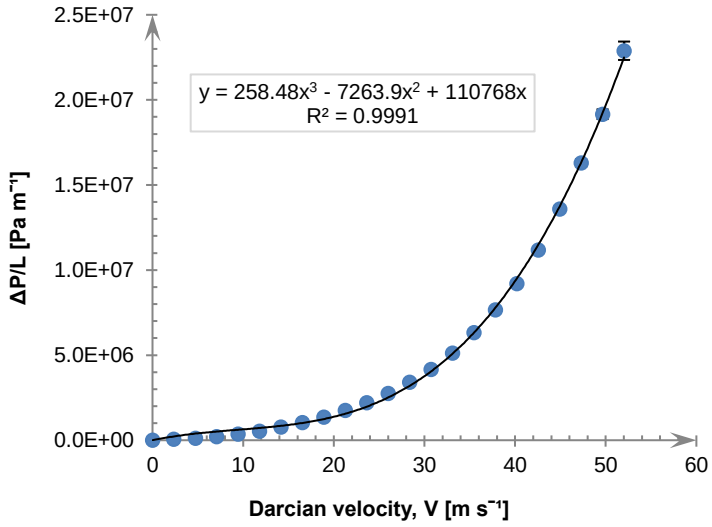

Fig. 4 Third order representation of ΔP/L vs. Darcian velocity for 20mm A-450 sample

The different regimes can be identified by using a graphical separation method used by Boomsma *et al* [11] and adopted in many related works [4, 6, 9, 13, 15, 16]. Figure 5 shows the various regimes and transitional regions including the commonly-studied Forchheimer regime, which was found to lie between 4 and 12 m s^{-1}. Table 2 identifies the regimes (according to [9]) more clearly, giving the approximate velocities at which they occur.

Table 2 Different regimes and corresponding velocity ranges

Regime	Velocity range (m s^{-1})
Darcy	0 - 4
Forchheimer	4 -12
Transitional	12 - 19
Turbulent	19 - 24
Post-turbulent I	24 - 31
Post-turbulent II	31 - 38

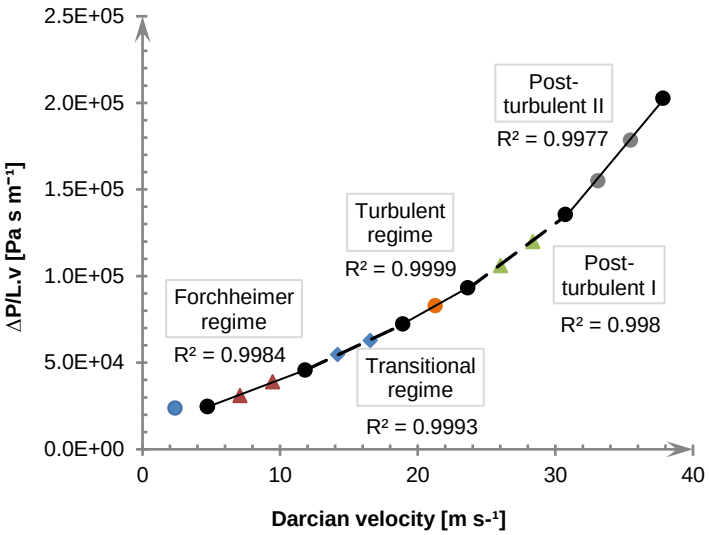

Fig. 5 Plot of ΔP/LV versus Darcian velocity for a 20mm thick, A-450 sample showing the different regimes

I. Effect of foam thickness on pressure-drop:

Pressure-drop values normalised by the sample thickness are plotted as a function of air flow velocity in Fig. 6. The apparent trend seems to be higher normalised pressure drops, at higher velocities, for thicker samples. The inset figure, detailing the behaviour at lower flow velocities, does not support this tendency, showing that no clear trend is maintained across the entire velocity range studied.

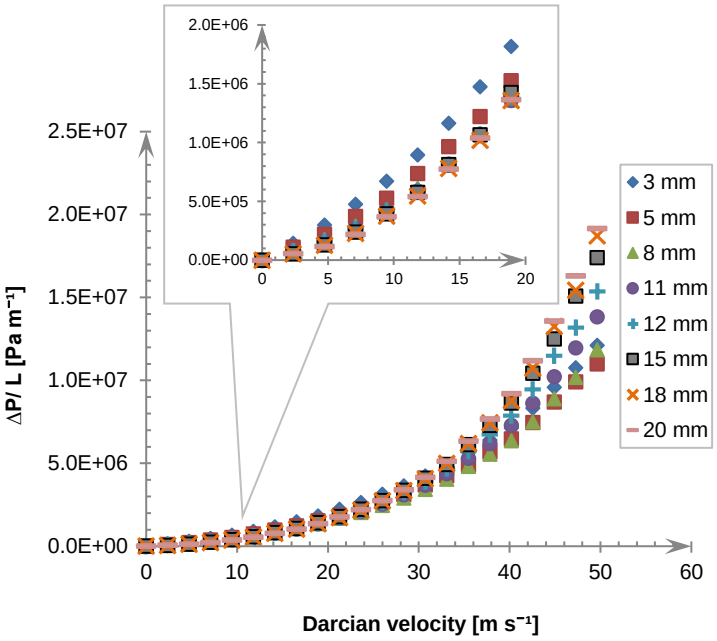

Fig. 6 Length-normalized pressure-drop vs. Darcian velocity for different thicknesses.

More detailed analysis of the data at the lower velocity range (coinciding with the Darcy, and Forchheimer regimes) is presented in Fig.7. For a given flow velocity, after an initial decrease in normalised pressure drop with thickness, for thicknesses greater than approximately 8-10 mm the normalised pressure drop, within experimental error, is independent of sample thickness. This "critical thickness" has been reported in several other studies and is a function of the pore size. Typically, thickness-independent behaviour is observed in the laminar flow region for flow distances exceeding 40-50 pore diameters [3, 9].

For air flow velocities exceeding the laminar flow regime (Darcy–Forchheimer regime) into the transitional and subsequent turbulent and post-turbulent regions (Fig. 8), the pressure drop-thickness relationship shows a minimum for thicknesses in the region of 7-10 mm, increasing with increasing thickness for thicknesses beyond this. As the air flow velocity increases, the entrance effect of distorted flow patterns develops across the sample until it covers the whole structure at which the downstream pressure transducer (Fig. 2) starts sensing pressure readings rather than atmospheric, with a significant increase in the upstream point, causing the pressure drop to be higher for thicker samples.

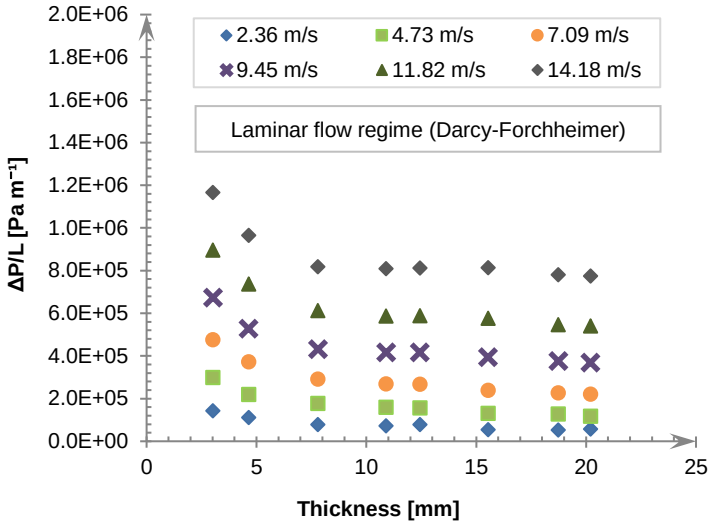

Fig. 7 Length-normalized pressure-drop vs. sample thickness at Darcian velocity up to 14 m s^{-1} covering both Darcy and Forchheimer regimes

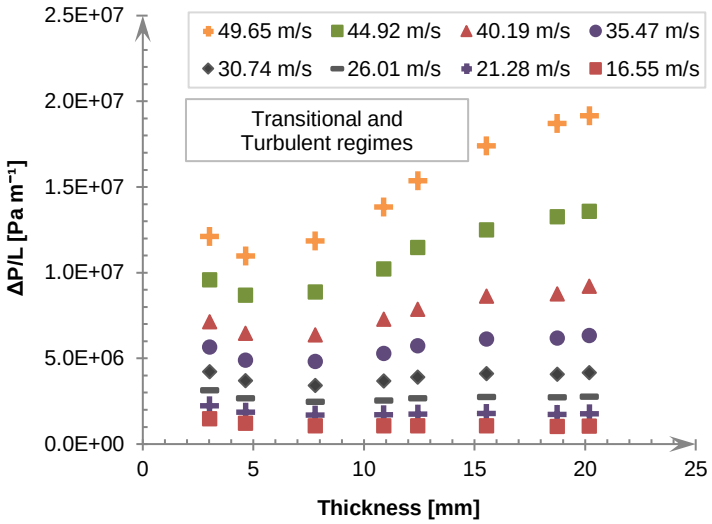

Fig. 8 Length-normalized pressure-drop vs. sample thickness at different Darcian velocities covering transitional, turbulent and port-turbulent regimes

II. Effect of porous metal stacking on pressure-drop:

Pressure-drop measurement across a multi-layered porous metal structure was carried out, comparing the behaviour for a stack of two 10 mm thick discs (10-10 mm) with that for single 10 and 20 mm thick samples. Figure 9 presents the length-normalised pressure drop values for these three configurations as a function of the Darcian velocity as well as the mathematical sum of the pressure drop for two, 10mm thick discs.

At lower air velocities, below 16 m s^{-1}, covering both the Darcy and Forchheimer regimes, the two solid samples behave in broadly the same manner, which is to be expected given that the flow conditions dictate thickness-independent behaviour for samples thicker than 8-10 mm. The stacked structure (10-10 mm) shows an average 10% increase in the pressure drop due to the misalignment of the discs, generating a discontinuity in the porous structure. At higher velocities (corresponding to transitional and turbulent regimes), thickness independence, as witnessed in the previous section, is no longer observed and the effect of an additional interface (for the stacked sample) is much more significant (a 10 to 20 % increase) an effect also reported in [3].

Mathematical addition of the individual pressure drop values for 10 mm thick samples gives pressure drops that are higher than all the other samples across the entire velocity range, since by summation, the entrance effect is (incorrectly) considered twice.

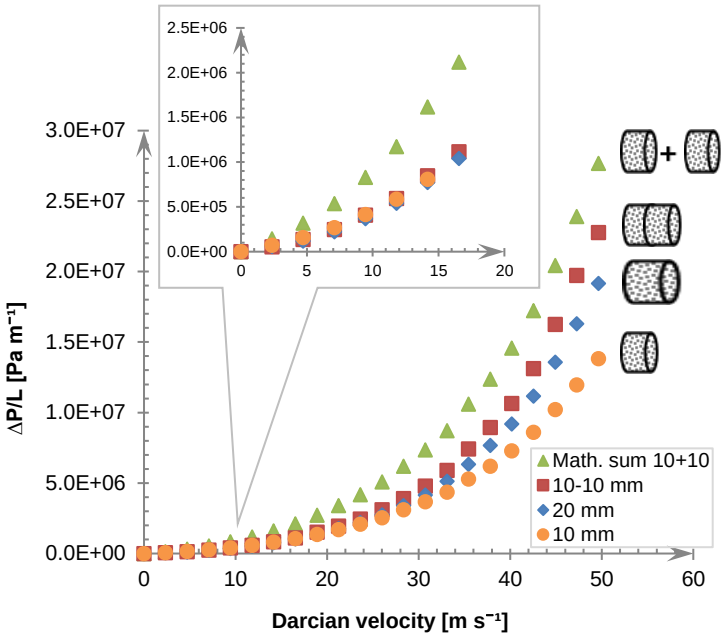

Fig. 9 Length-normalised pressure drop vs. Darcian velocity for 20mm and 10mm A-450 samples, a stack of two 10mm A-450 discs and mathematical summation of pressure drop values for two 10mm A-450 samples +

III. Effect of air-gap on pressure-drop:

Figure 10 presents the normalised-pressure drop versus Darcian velocity relationship for porous metal structures with an air gap, compared with 10 and 20 mm bulk samples and a stack of two 10 mm discs, 10-10 mm (now called 0 mm gap). A total metal thickness of 20 mm was used to calculate the normalised pressure drop for all structures with gaps. Having an air gap increases the pressure drop but increasing the gap size, from 2 mm to 10 mm, doesn't alter the pressure drop significantly even over the entire velocity range (which is within the uncertainty limits of the experiment conducted). A more focused analysis at 14 m s^{-1} reveals that the normalised pressure drop values for stacked porous structures with no air gap (8.48 x 10^5 Pa m^{-1}) and with a 6 mm air-gap (9.55 x 10^5 Pa m^{-1}) are 10 and 23 % higher than the bulk (20 mm) sample (7.74 x 10^5 Pa m^{-1}). At 50 m s^{-1}, these increases are 19 and 37 %, respectively (reaching 2.64 x 10^6 Pa m^{-1}). The pressure drop increase, compared to the stack of two 10 mm and 10 and 20 mm bulk samples, can be attributed to the additional entrance/exit effect developed by the addition of a new surface as reported in [3].

It should be noted that for air velocities exceeding 12 m s^{-1}, the normalised pressure drop for porous structures with air gaps exceeds the mathematical summation of the pressure-drop values for two 10mm samples, suggesting that flow disturbances generated within the air gap at higher velocities also contribute to the pressure drop.

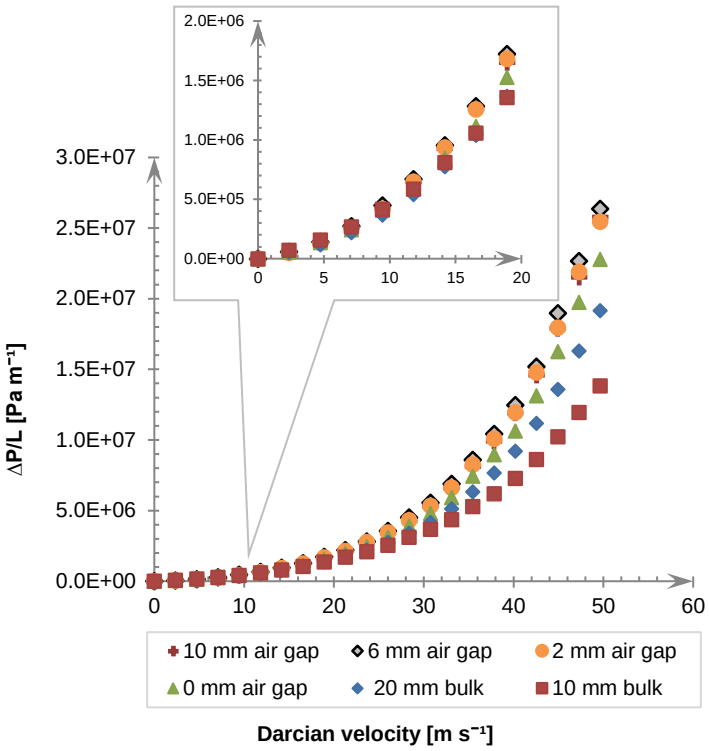

Fig. 10 Normalised- pressure drop vs. Darcian velocity for two 10mm A-450 discs with four different air gap sizes and 10 and 20 mm A-450 bulk samples

Since, as was shown in Fig. 7 and 8, the 3 mm thick porous metal delivers the highest pressure drop per unit length, over an approximate velocity range of 0 to 30 m s^{-1}, this behaviour could be exploited to create "material-efficient" structures which exhibit high pressure drops by using multiple, thin porous metal sheets. Figure 11 shows the length-normalised pressure drop as a function of the Darcian velocity for a 9 mm bulk sample, a stack of three (misaligned) 3 mm discs (3-3-3 mm), and a porous structure of three 3 mm discs separated by two 3 mm air gaps (3||3||3 mm), all with the same mass of 3.38 g. The length dimension used to determine the normalised pressure drop is for the thickness of porous metal only. At 14 m s^{-1} the normalised pressure drop value for gapped structures is 17% higher than for the bulk (9 mm) sample and at 50 m s^{-1}, this increases to 43% (to 1.69 x 10^7 Pa m^{-1}).

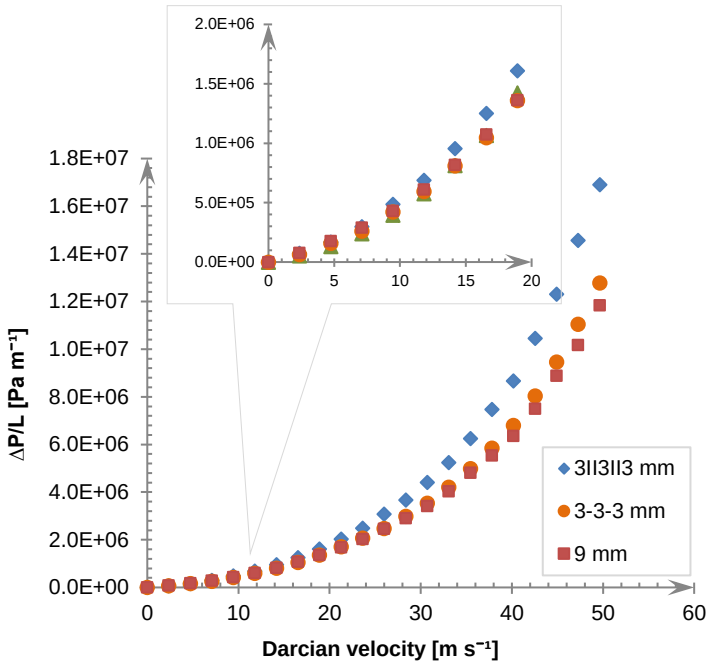

Fig. 11 Normalised- pressure drop vs. Darcian velocity for a stack of three 3mm discs with 3mm air gaps in between and without air gaps in comparison with 9 and 15mm A-450 bulk samples

4. Conclusions

The pressure-drop characteristics for novel, multi-layered Inconel porous structures have been investigated for an airflow velocity range of 0-50 m s^{-1}. Third order polynomial regression curve provides the best fit to the length-normalized pressure drop versus Darcian velocity data and a graphical separation method enables the identification of numerous flow regimes.

For an air velocity range corresponding to the Darcy and Forchheimer regimes, the independence of normalised pressure drop on thickness was noticed for samples thicker than roughly 8 mm. This relationship was not preserved at higher airflow velocities.

Entrance and exit effects are highlighted as a source of the pressure-drop increase for porous structures with air gaps, regardless of their sizes, as long as they are bigger than those generated by loosely-stacked structures. The pressure-drops for gapped porous structures and the mathematical-summation of the pressure drop for the corresponding individual components, were in very good agreement, at lower airflow velocities.

The potential for mass-efficient porous structures, providing a high pressure-drop, was demonstrated using multiple thin porous laminates (of thickness below the critical thickness for length independence of pressure drop), separated by air gaps.

NOTE: Ethical standards

I declare that the experiments in the manuscript submitted comply with the current laws of the United Kingdom.

References

1. N. Dukhan, Exp. Fluids 41, 4665-4672 (2006)
2. M. Medraj, E. Baril, V. Loya, L.P. Lefebvre, J. Mater. Sci. 42, 4372–4383 (2007)
3. E. Baril, A. Mostafid, L.P. Lefebvre, M. Medraj, Adv. Eng. Mater. 10, 889–894 (2008)
4. S. Mancin, C. Zilio, A. Cavallini, L. Rossetto, Int. J. Heat Mass Transf. 53, 3121–3130 (2010)
5. W. Azzi, W. Roberts, A. Rabiei, Mater. design. 28, 569-574 (2007)
6. N. Dukhan, C. Minjeur II, J. Porous Mater. 18, 417–424 (2011)
7. N. Dukhan, Metal Foams: Fundamentals and Applications (Destech Publications, Lancaster, 2013), pp. 31–45
8. D. Ingham, I. Pop, Transport Phenomena in Porous Media, 1st edn. (Elsevier Science, Oxford, 1998)
9. H. Oun, A. Kennedy, J. Porous Mater. 21, 1133-1141(2014)
10. P. Khayargoli, V. Loya, L.P. Lefebvre, M. Medraj, Presented at the CSME Forum (Can. Soc. Mech. Eng., Ontario, 2004)
11. K. Boomsma, D. Poulikakos, ASME J. Fluids Eng. 124, 263–272 (2002)
12. C.Y. Zhao, T.Kim, T.J. Lu, H.P. Hodson, Thermal transport phenomena in Porvair metal foams and sintered beds. (Fuel Cell Markets web,2001), http://www.fuelcellmarkets.com/fuel_cell_ markets/1,1,1.html. Accessed 26 Mar 2013
13. N. Dukhan, M. Ali, Presented at the 7th international conference on porous metals and metallic foams (BEXCO, Busan, Korea 2011)
14. O. Gerbaux, T. Vercueil, A. Memponteil, B. Bador, Chem. Eng. Sci. 64, 4186–4195 (2009)
15. N. Dukhan, K. Patel, Presented at the 3rd international conference on porous media and its applications in science, engineering and industry (The II Ciocco Hotal and conference centre, Tuscany, Italy, 2010)
16. N. Dukhan, M. Ali, Int. J. Therm. Sci. 57, 85–91 (2012)